Chapter 6: CGRS Lineaments and geomorphology of Northern California

Abstract

Eight directions of small circle lineament trends are traced in three locations of the surface topography of California. They are shown to be consistently visible at various altitudes and terranes and extend the entire dimensions of the state. In finding a cause for these shears the linears are compared to direction of accretion reflected in continental edges and mapped faults. Neither provide a consistent correlation. They do exhibit small circle relationships, and can be associated with recognized shear centers. Classified as Concentric Global Ring Structures, I postulate their genesis relates to changes from the stress at these centers.

Key Words: Lineaments, Concentric Global Ring Structures, geomorphology, erosion.

Introduction

The previous chapters have explored one set of linears through the Pacific Ocean, commonly called the Pacific Fracture Zones. These linears are identified as Concentric Global Ring Structures (CGRS) and are Trend 3 in this chapter. They are one of eight trends that are traced as CGRS across California and are related to their global centers. This was not possible for early photogeologist. H.N. Fisk, from 1944-1947 laid his 23 x 23cm (9 x 9 in) images out on a college gym floors (Gay 2012), as he tried to find the source of the shear that produced linear trends. Google Earth, with its satellite sourced images, expand the search from gym floor size to global. Google Earth is a highly productive tool for this using a program designed by Maarten ‘t Hart (personal communications) that calculates and draws circles on the globe using a rim point and the provided center.

Gay (2012, page 10) draws the conclusion, “On cratons, joints, linears and lineaments, as well as fractures and faults, result from reactivation of pre-existing faults/shear zones in the underlying Precambrian basement.” The epoch given, Precambrian, is a presupposition, and the connection from the basement to the top of the sedimentary heap is an assumption, but mapping these linears on the surface does indicate deep structures. Concentric linears “are aligned in … slightly curvilinear relationship, and which differs distinctly from the pattern of adjacent features” (as lineaments are defined by O’Leary and Friedman, 1978 (quoted in Tiren 2010). When considering the scope of linears presented, Gay’s (2012) statement, “to not attempt to understand lineaments is to ignore one of the most common and basic features in geology (page 3)," or R.A. Hodgson (1961), “Lineaments could be a clue to the elusive orientating mechanism for systematic regional joints in undeformed sedimentary rocks.” seems especially pertinent.

This paper will correlate these liner trends with Concentric Global Ring Structures (CGRS) which together with the strongly curvilinear lineaments (Barnhart 2017) determined the geomorphic shape of Earth’s topography and bathymetry.

Methods

Recognizing Lineaments

Figure 6.1 demonstrates that linears can be viewed on Google Earth at various zoom levels. Under the red line starting from the west edge, the dark crack prior to the “twisted” ridge, grooves in the snow cover of Thompson Peak (TP), a narrow bridge between Thomas Peak and Little Granite Peak (LGP) and a “fin” protruding to the east of Little Granite Peak is a linear. The other “twisted” ridges with the valleys between them and additional bridges and fins marked with red arrows (trend 7) indicate additional linears parallel to the first linear/red line. The white line indicates a linear over the eastern edge of the rounded form protruding southeast from Little Granite Peak and the deep canyon that divides it from the angular shaped rocks to its east. The lineament continues into grooves on the top of Little Granite Peak. Pairs of single sided white arrows (trend 1) indicate additional linears that are parallel to the white line. Two pair of double sided yellow arrows (trend 8) indicate two dark valley linears that are parallel to each other, near the east and west edges of the image. All of these are the type of linears discussed in this paper and two or more linears headed in the same direction are grouped as a trend. Once drawn, the bright lines distracts the eye in its immediate vicinity, so readers are encouraged to use Google Earth for themselves to view linears first hand. There are many more visible, and the recognition of multiple concentrically repeated units with regular spacing provides confidence in the designation of lineaments (Chapter 2).

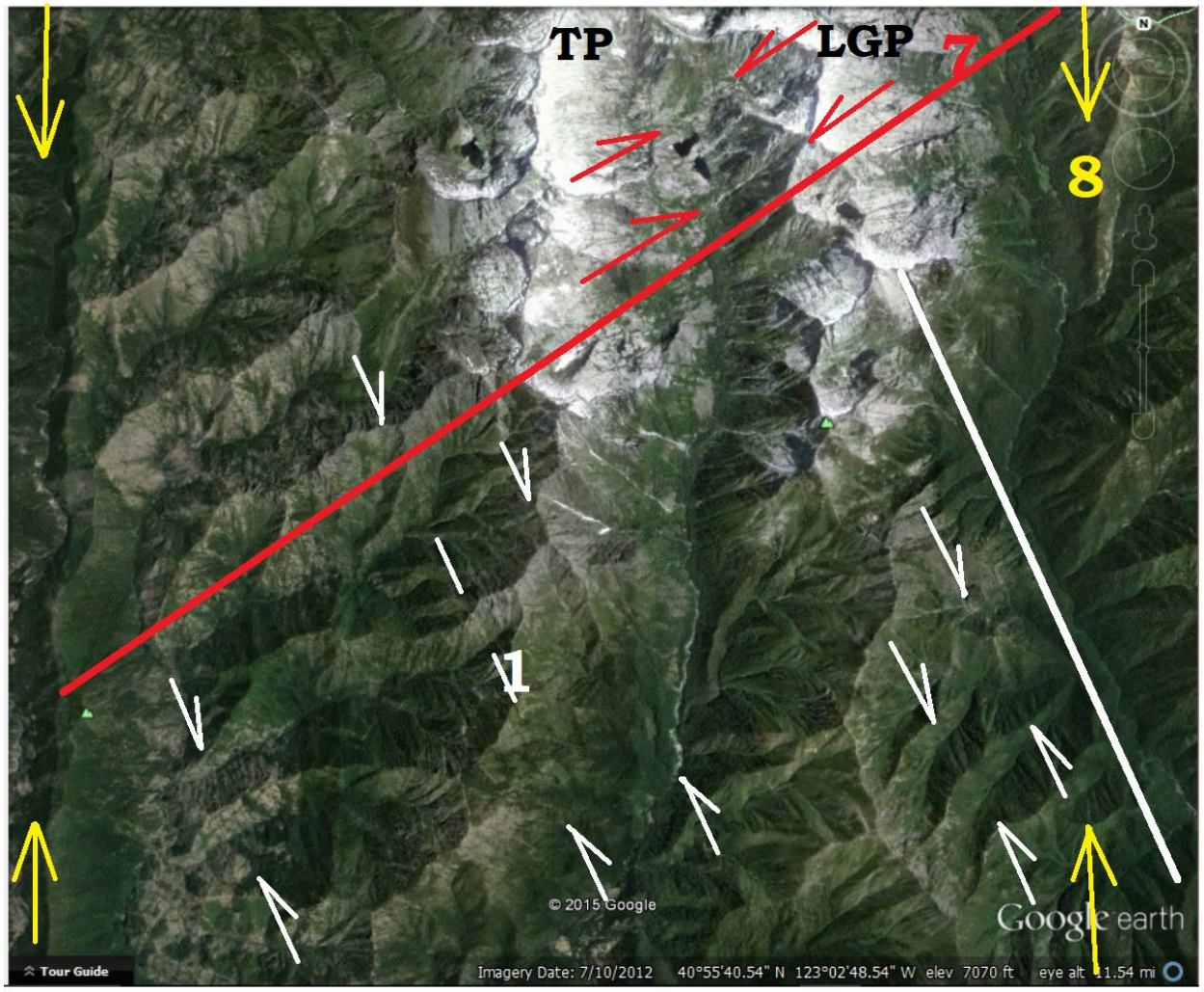

Figure 6.1: Google Earth image of Thompson (TP) and Little Granite Peaks (LGP) in the Klamath Mountains. Three sets of linear trends are indicated by the three different colors. Image is a detail near the center of Figure 3. (2012. 40º55'40.54"N, 123º02'40.54"W, accessed 20 April 2016.)

This paper will document three locations in Northern California; (A) Redding with the Klamath and Cascade Mountains, (B) Mount Lassen and the Feather River Valley, and (C) the Williams to Dunnigan section of the Coastal Range (Figure 6.2). To demonstrate whether random or nonrandom arrangement of mountain building and erosion exist, linears in each area will be charted. If trends exist, then they are not random. If they are nonrandom, do they conform to lithology and current fault consistent with accretion through plate tectonics? Or, do linear trends conform to Small Circles, with mappable centers as the CGRS model (Chapter 3) posits?

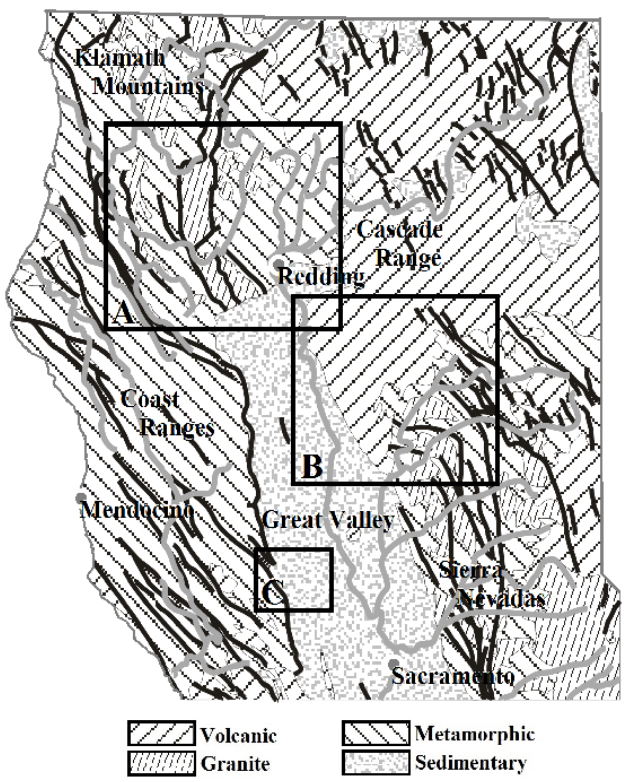

Figure 6.2: Generalized geology of Northern California showing the location of the primary lithology, geomorphic provinces, and faults believed to control that morphology. The three areas that will be considered are indicated with the relative size of each. (A) Redding with Klamath and Cascade Mountains (Figure 6.3), (B) Mount Lassen and the Feather River Valley (Figure 6.9). (C) Williams to Dunnigan section of the Coastal Range (Figure 6.16). (Map after Wampole (2006).

Redding with Klamath and Cascade Mountains

Klamath Mountains

The Klamath Mountains are characterized as great arcs opening to the east (Wampole 2006) composed of repeated layers of metamorphic rocks and granite, Figure 6.2. The metamorphics are from "volcanic and sedimentary rocks that represent volcanic island arcs, submarine plateaus, reef-like bodies of limestone, and deep ocean sediments." Many are identified as ophiolites accreted to the continental edge, as early as 600 million years ago (DeCourten 2015, page 12). For the Klamath Mountains to accrete, linears parallel with the lithology's form, or parallel to the coast, or associated in the direction of thrust, from southwest to northeast (Figure 6.2) are expected. This thrust is parallel to 7 but perpendicular to trend 1 (Figure 6.3.7 & 5.3.1). Accretion cannot produce both.

Southern Cascade Range

Having a surface of mostly basaltic origin (DeCourten 2015, page 25-27), the southern edge of the Cascade Range is a much larger physiographic province, Figure 6.2, that extends all the way up to British Columbia. As the Klamath Mountains are composed of similar lithology to the Sierra Nevada, granite alternating with metamorphic, there is some possibility that the basalts of the Cascades are only a cover over a basement structure that is similar to the Klamath province and connects them with the Sierra Nevada (DeCourten 2015, page 14). This may be true, as lineament 1 also defines the trend of the Sierra Nevada (Figure 6.18).

Central Valley Sequence

The Central Valley is a lowland between hills and mountains on both long sides. As such the valley floor is covered with a sequence of alluvium. In it continuously shifting, meandering rivers left "heterogeneous assemblages of channel gravels, river bank sands, silt, and clay deposited on the broad floodplain, and in some places, peat deposits represent plant litter that accumulated in lakes and wetlands," according to DeCourten (2015, page 14). Instead of "continuously… meandering rivers." The study of the Coastal Range (See Chapter 17) shows a onetime event connected with the impact of the Mendocino crater.

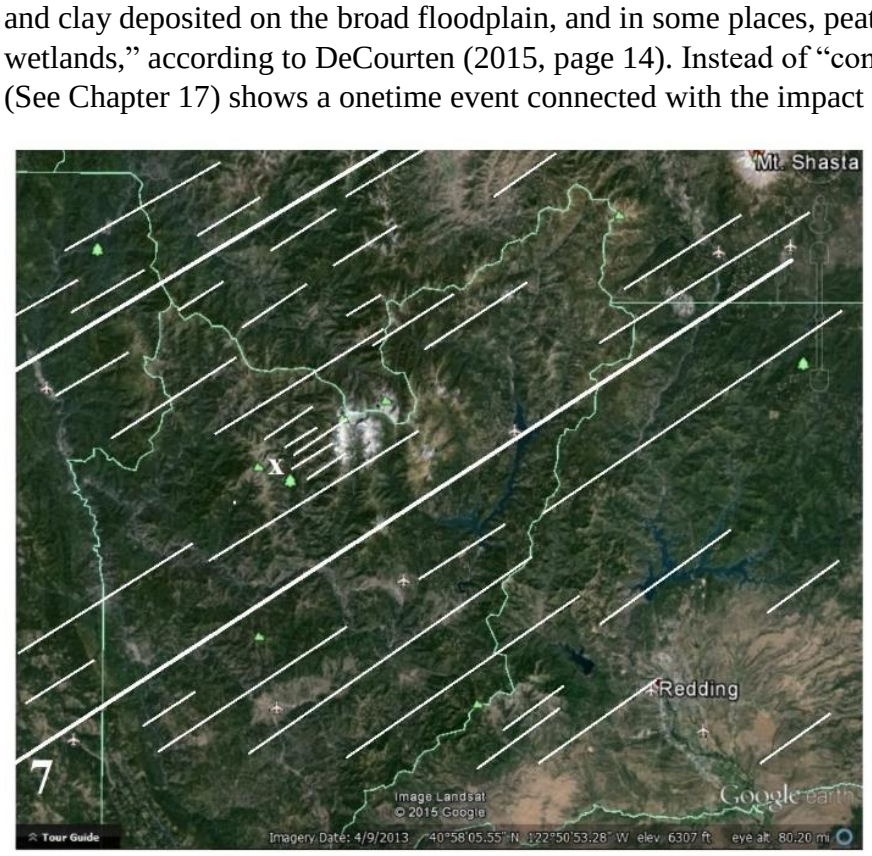

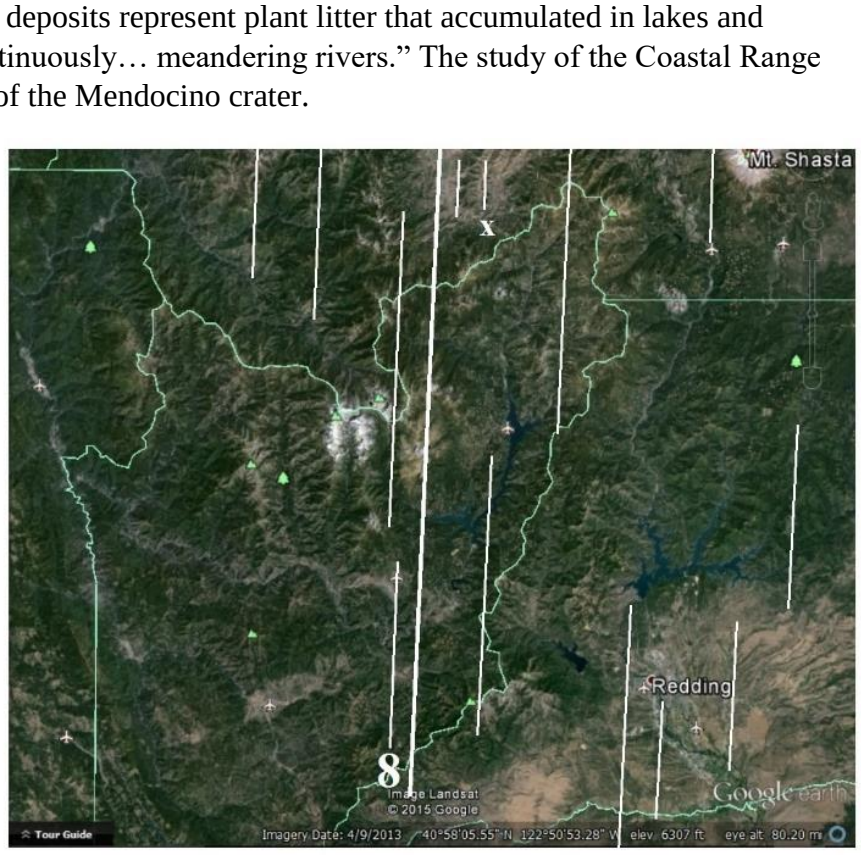

Figure 6.3. Google Earth image of Redding, California with the northern end of the Coastal Range to the west, Klamath Mountains to the northwest, and Cascade Mountains to the east and north, including Mount Shasta. Image 6.3.1: Select linears concentric to trend 1. Image 6.3.2: Select linears concentric to trend 2. Image 6.3.3: Select linears concentric to trend 3. Image 6.3.4: Select linears concentric to trend 4. Image 6.3.5: Select linears concentric to trend 5. Image 6.3.6: Select linears concentric to trend 6. Image 6.3.7: Select linears concentric to trend 7. Image 6.3.8: Select linears concentric to trend 8. (2013. 40˚58'05.55"N, 122˚50'53.20"W, accessed 20 December 2015.)


Mt. Shasta
x
Redding
1
Image Landsat
© 2015 Google
Google earth
Tour Guide
Imagery Date: 4/9/2013 40°58'05.55" N 122°50'53.28" W elev 6307 ft eye alt 80.20 mi


Mt. Shasta
Redding
2
Image Landsat
© 2015 Google
Google earth
Tour Guide
Imagery Date: 4/9/2013 40°58'05.55" N 122°50'53.28" W elev 6307 ft eye alt 80.20 mi


Mt. Shasta
Redding
3
Image Landsat
© 2015 Google
Google earth
Tour Guide
Imagery Date: 4/9/2013 40°58'05.55" N 122°50'53.28" W elev 6307 ft eye alt 80.20 mi

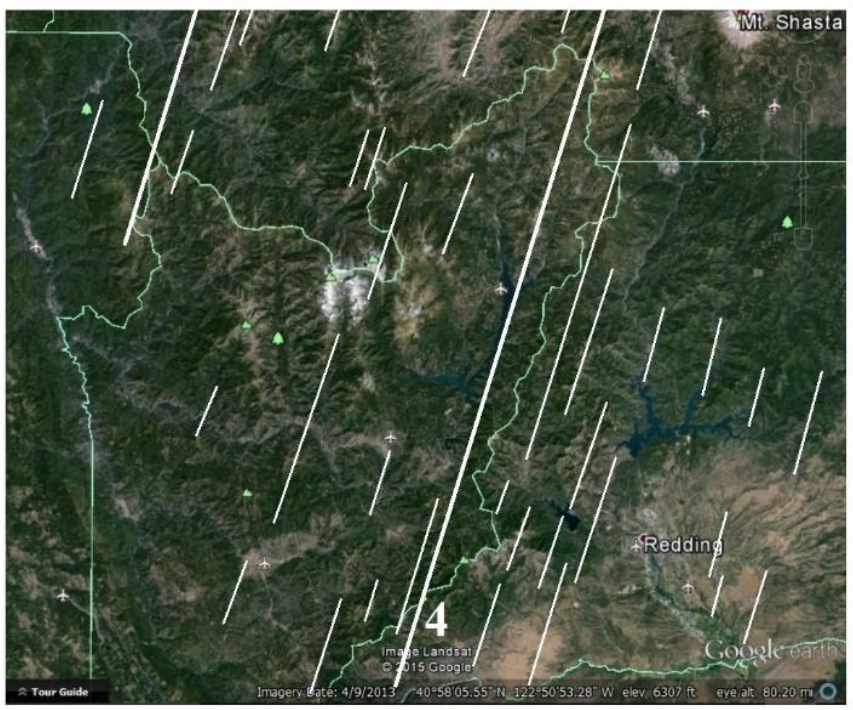
Mt. Shasta
Redding
4
Image Landsat
© 2015 Google
Google earth
Tour Guide
Imagery Date: 4/9/2013 40°58'05.55" N 122°50'53.28" W elev 6307 ft eye alt 80.20 mi

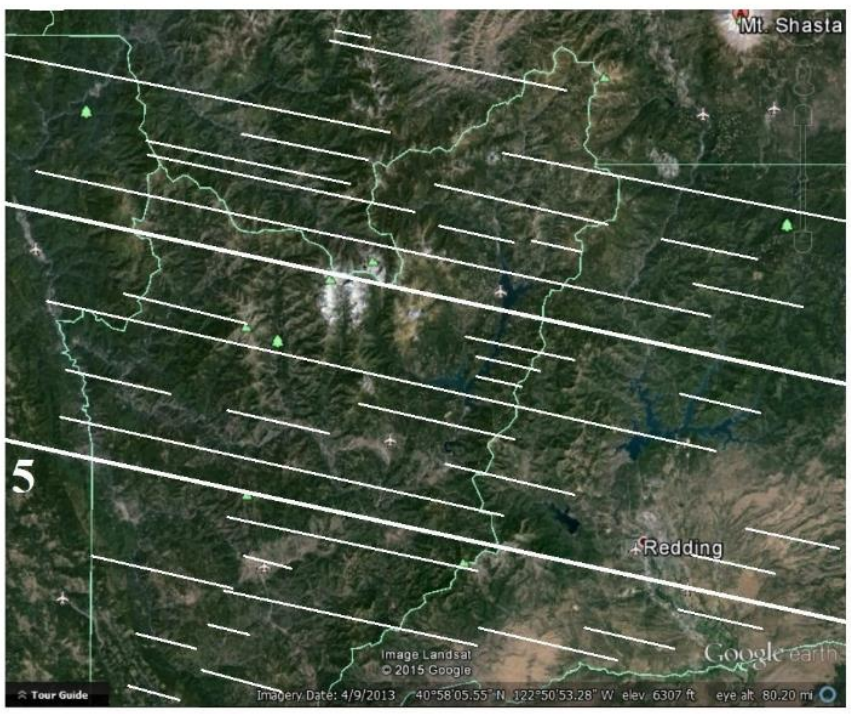
Mt. Shasta
Redding
5
Image Landsat
© 2015 Google
Google earth
Tour Guide
Imagery Date: 4/9/2013 40°58'05.55" N 122°50'53.28" W elev 6307 ft eye alt 80.20 mi

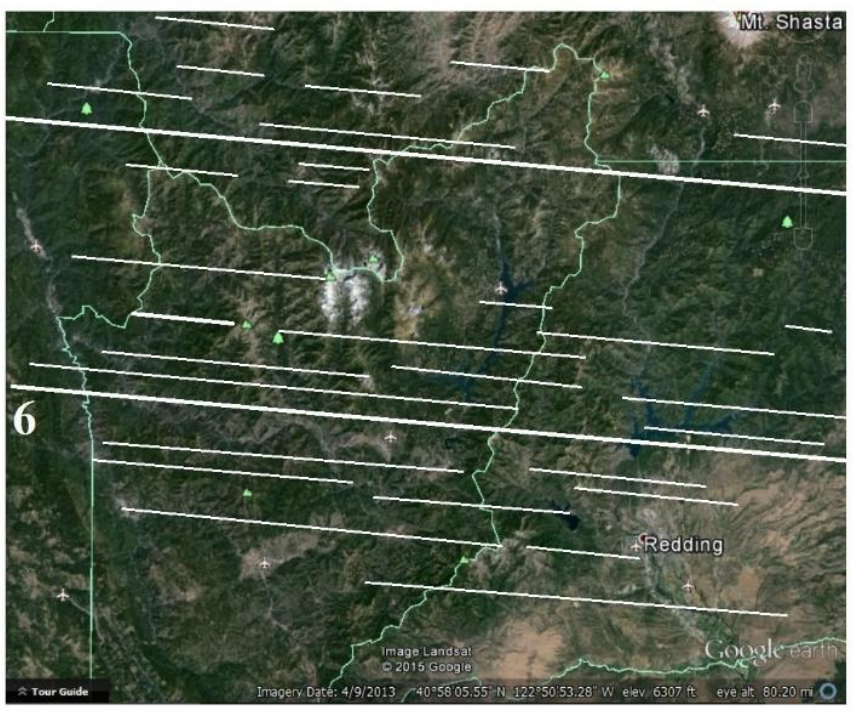
Mt. Shasta
6
Redding
Image Landsat
© 2015 Google
Google earth
Tour Guide
Imagery Date: 4/9/2013 40°58'05.55" N 122°50'53.28" W elev 6307 ft eye alt 80.20 mi

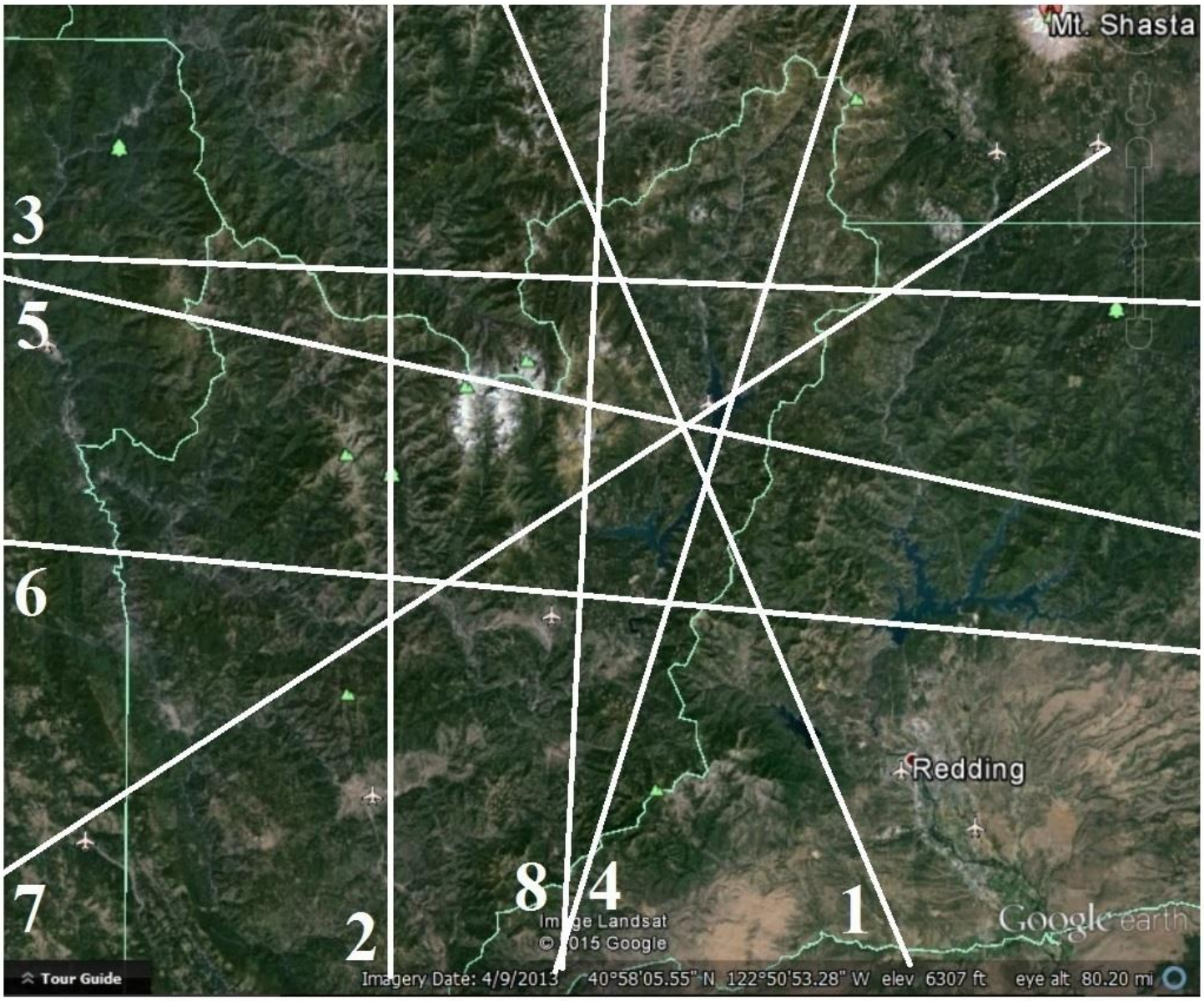

Figure 6.4. Google Earth image of Redding, California showing a compilation of 8 lineaments indication direction of trends. (2013, same as Figure 6.3.)

The eight lineaments of the Redding area are charted in Figure 6.3.1- 6.3.8, with Figure 6.4 showing the comparative angles of the individual trends, verifying they are all unique. A careful observer of any of the separate images will note that less than half of the possible linears are marked for each trend, and not all possible trends are represented by these 8, but yet, the angles are not varied enough that possible trends are infinite.

Considering these lineaments in Figure 6.4, it is evident that not all of these trends can be consistent with limited tectonic movement in the area unless additional lineaments were inherited from earlier motion and collisions of the block, as was suggested by O'Driscoll (1983). However, if these lineaments were inherited, we would not expect them to be continuous over all of California.

Lineaments might be determined by faulting in the area. Figure 6.2 shows some of the major trends of faulting, and Figure 6.5 shows the major faults specific to this area. Those on the lower right of Figure 6.5 align with trend 7 (compare with Figure 6.4), while those in the upper right align with trend 1. Yet, those in the left half do not seem to align with any lineament in Figure 6.4. They are arced and a careful examination of that area in Figure 6.3 will show similar strongly curvilinear lineaments in the lithology. These are the great arcs opening to the east of the Klamath Mountains (Wampole 2006). DeCourten (2015) connected these to the accreting edge of the continent, generated here by the subduction of the Juan de Fuca plate bordered on the south by the Mendocino fracture zone extending to the Feather River Valley of the northern Sierra Nevada (Figure 6.9).

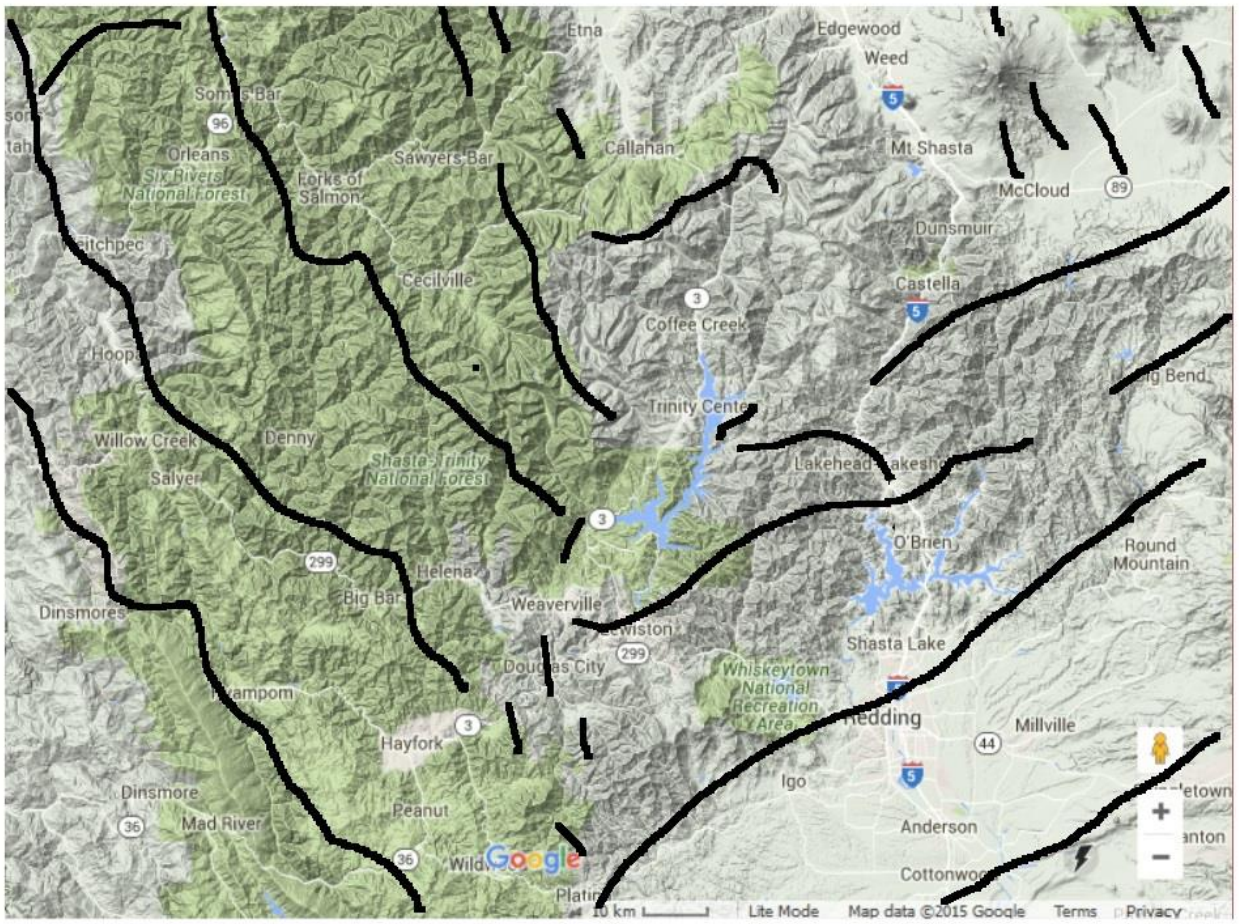

Figure 6.5. Google Earth Terrain map of same area as figure 3 showing the major faults and fault trends. (After Gutierrez et al 2010.)

It is one thing to see linears in the vertical view, but are they recognizable from a horizontal view? Figures 6.6, 6.7 and 6.8 view the ridges and gullies that compose the eroded surface. With a topographic drape, the variation of vegetation is sheared off the topography, making slight variations of structure more visible.

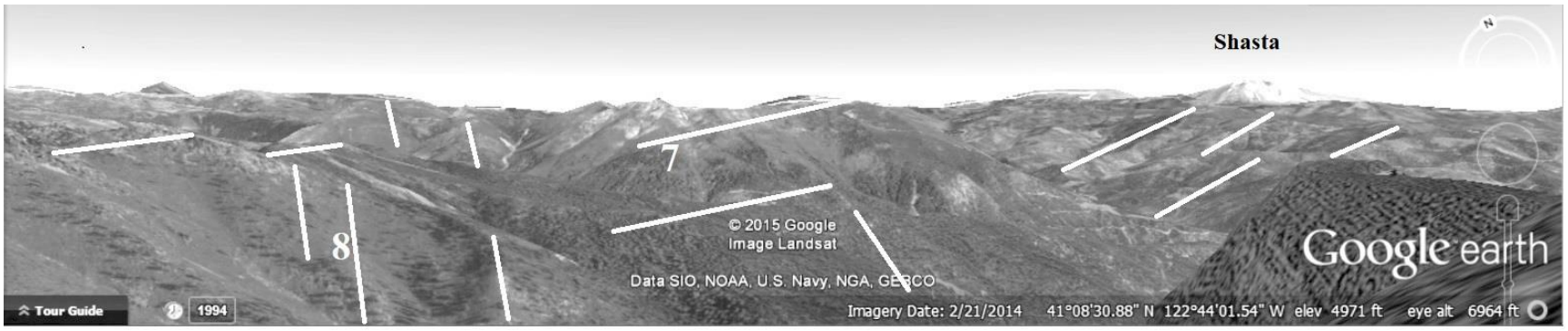

Figure 6.6. Google Earth Topographic drape of Cascade Mountains looking east of north towards Shasta Mountain at point x, Figure 6.3.1. Ridges align in midground to Figure 6.3.7, and shift midway aligning with trend 1. (2014. 41˚17’41.22”N. 122˚45’45.38”W, accessed 20 December 2015.)

Anything naturally produced contains a certain amount of limited irregularity (as seen repeatedly on the moon from additional cratering interaction) distinct from randomness. Looking at any of the erosional channels in Figure 6.6 and the gully oscillates left and right in an irregular manner, as they connect with the primarily parallel dendritic pattern of erosion off the ridges. Yet, study of the arrangement of the primary and side ridges between the parallel dendrites show their linear form, suggesting some random difference in the *extent*, but not *placement* of erosion. Figure 6.7 shows similarity on trend 1 but noncontinuous expression of trend 7. The single point arrows on the left show a repeated pattern and the double pointed arrows on the right show a different repeated pattern.

Figure 6.7 demonstrates the consistent tendency to follow a pattern when the adjacent ridges not only express parallel linears, but those linears turn from the orientation of one to the alignment of a second linear at adjacent points. This manner of linear intersection is consistent with the mapping of fault linears by Gay (2012) with abrupt corners at their junctions.

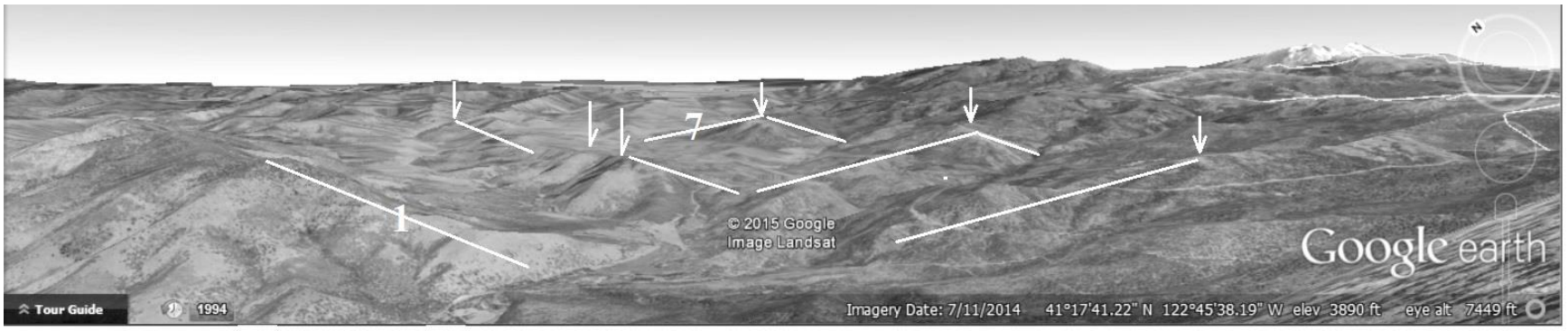

Figure 6.7. Google Earth Topographic drape of Cascade Mountains looking northeast towards Shasta Mountain, at point x, Figure 6.3.8. Major ridges are trend 7 with small intervening ridges with trend 1 in multiple ancillary patterns. (2014. 41˚17'41.22"N, 122˚45'30.19"W, accessed 20 December 2015.)

Figure 6.8 shows at least five long ridges, 14 km (8.5 miles) long, interspersed with two shorter ridges on the right, yet all are parallel. That this would happen randomly without some controlling fault system is remarkable. These lineaments on the map extend for 140 km (90 miles) in a slightly curvilinear lineament as they cross Figure 6.3. The consistent occurrence of linears seems improbable without some structural control or are the linears structural control for everything else?

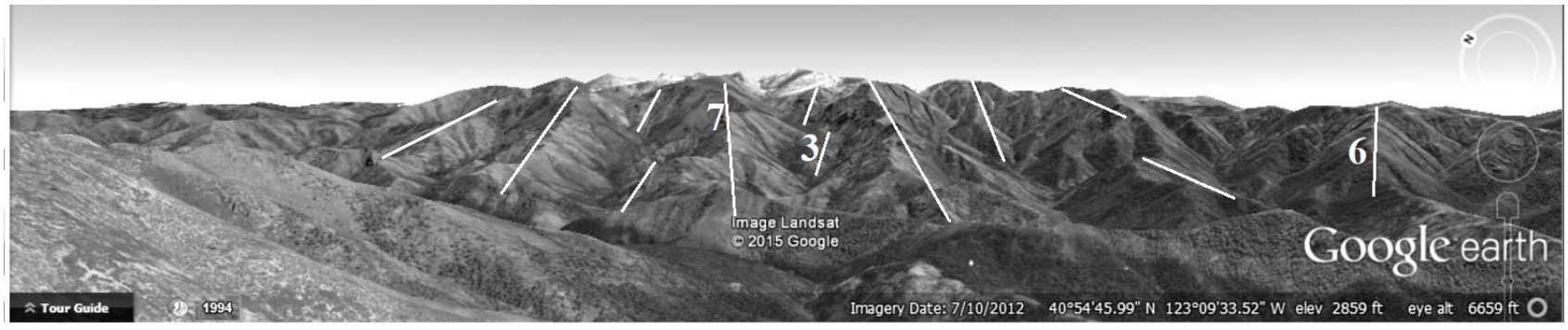

Figure 6.8. Google Earth Topographic drape of Klamath Mountains looking to northeast towards snow covered Thompson Peak. This is the view into the twisted ridges of Figure 6.1, from point x, Figure 6.3.7. Note alignment of most ridges through the center of the image, whether long or short, are parallel and align with trend 7, Figure 6.3.7, while most cross ridges of the slopes are aligned with trend 1, Figure 6.3.1. This alignment extends to the extreme foreground. (2012. 40˚54'45.99"N, 123˚09'33.52"W, accessed 20 December 2015.)

Mount Lassen and the Feather River Valley

Volcanoes of the Cascade Range

The Cascades are known for their volcanoes. Shasta, north of Redding, and Lassen, north of the Feather River Valley (Figure 6.10), Medicine Lake, further north in California, Crater Lake, Mount Baker, and Mount Hood in Oregon, and Mount Rainier and Mount St. Helens of Washington are all part of the Cascades.

Mount Lassen is the southernmost of these volcanoes and the Mendocino fracture zone is charted just south of it, where it conforms to trend 6, dividing the Cascades and Sierra Nevada Range.

Sierra Nevada Mountains

The core of the Sierra Nevada is a batholith of granite with metamorphics on both sides. Where it meets the south end of the Cascades it is rimmed on the west by metamorphic rocks attributed to oceanic origin that includes mafic magma and oceanic sediments "such as chert, mudstone and limestone that have been metamorphosed to varying degree" (DeCourten 2015, page 8). The rocks DeCourten describes do exist, but the linears do not fit the origin he describes for them.


Lassen Peak
Red Bluff
Chico
Paradise
1
Image Landsat
© 2015 Google
Google earth
Tour Guide
Imagery Date: 4/9/2013 40°04'32.62" N 121°31'38.88" W elev 5023 ft eye alt 72.74 mi


Lassen Peak
Red Bluff
Chico
Paradise
2
Image Landsat
© 2015 Google
Google earth
Tour Guide
Imagery Date: 4/9/2013 40°04'32.62" N 121°31'38.88" W elev 5023 ft eye alt 72.74 mi


Lassen Peak
3
Red Bluff
Chico
Paradise
Image Landsat
© 2015 Google
Google earth
Tour Guide
Imagery Date: 4/9/2013 40°04'32.62" N 121°31'38.88" W elev 5023 ft eye alt 72.74 mi


Lassen Peak
Red Bluff
Chico
Paradise
4
Image Landsat
© 2015 Google
Google earth
Tour Guide
Imagery Date: 4/9/2013 40°04'32.62" N 121°31'38.88" W elev 5023 ft eye alt 72.74 mi

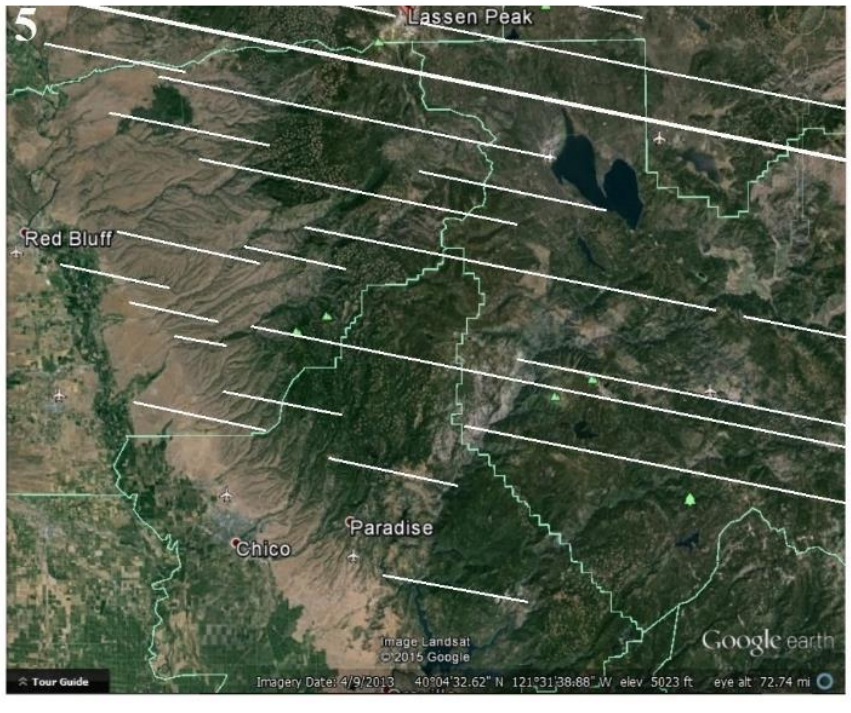
5
Lassen Peak
Red Bluff
Chico
Paradise
Image Landsat
© 2015 Google
Google earth
Tour Guide
Imagery Date: 4/9/2013 40°04'32.62" N 121°31'38.88" W elev 5023 ft eye alt 72.74 mi


Lassen Peak
Red Bluff
6
Chico
Paradise
Image Landsat
© 2015 Google
Google earth
Tour Guide
Imagery Date: 4/9/2013 40°04'32.62" N 121°31'38.88" W elev 5023 ft eye alt 72.74 mi

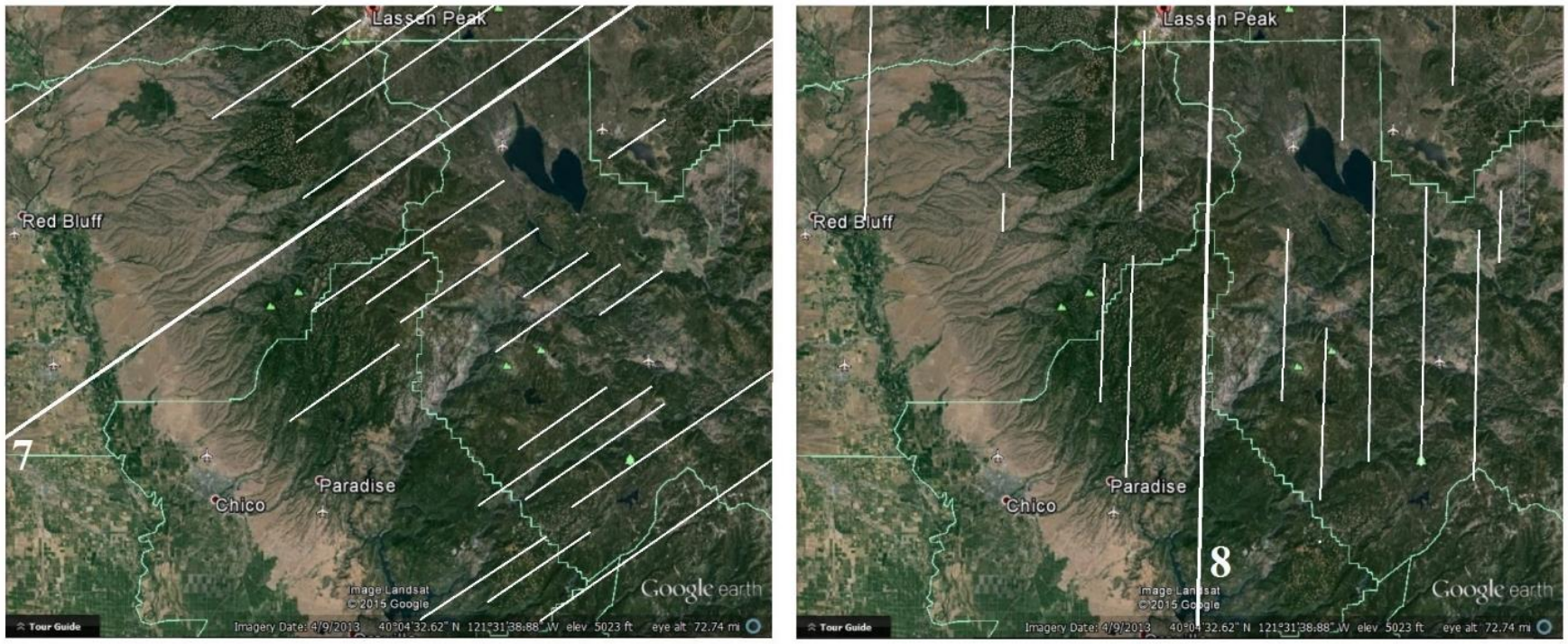

Figure 6.9. Google Earth image of Mount Lassen, California with the southern end of the Cascade Mountains and the northern end of the Sierra Nevada Mountains dividing at the Feather River Canyon, Figure 6.10. Figures 6.9.1- 6.9.8 explanations consistent with Figure 6.3. (2013. 40˚04'32.62"N, 121˚31'38.88"W, accessed 18 December 2015.)

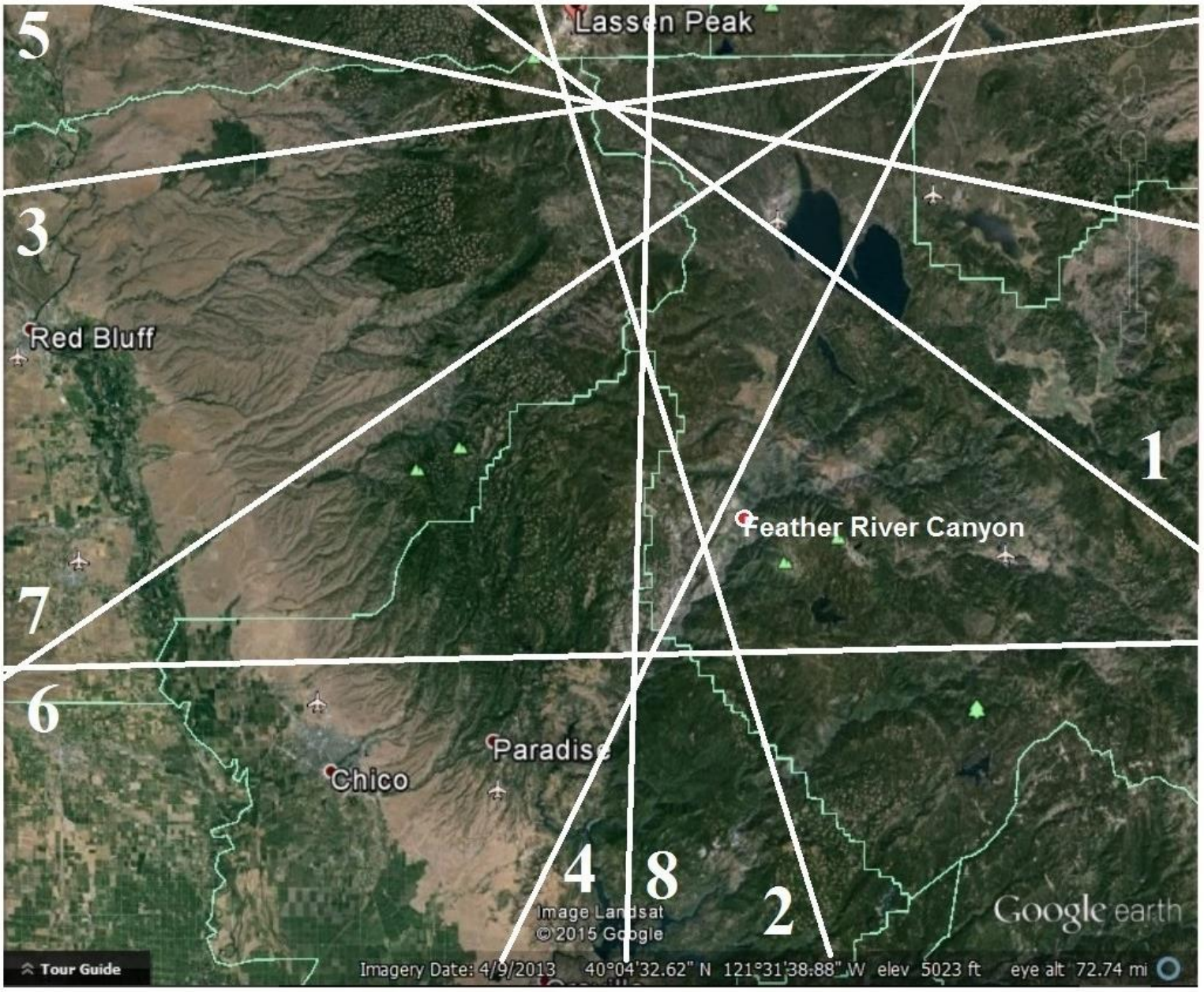

Figure 6.10. Google Earth image of Mount Lassen, California showing all 8 lineaments. (2013, same as figure 6.9.)

While all eight of the lineaments have many expressions in this area, trend 2 is the general direction of the Cascade's ridge. While Figure 6.10 does not go far enough south to really show it, the trend of the lower valley, parallel to the Sierra Nevada, below Feather River Valley, is trend 1 (see Figure 6.18). While these two trends may express the general direction of the mountain ridge, the expression of the other six lineaments are not diminished in this area.

Looking at a fault map of the same area, Figure 6.11, we see 5 small faults at the very top of the image that align with trend 2, and a number to the lower left in the foothills that align with trend 1. There are a few scattered about that align with trend 7, but then a majority of the faults in the upper right seem to form in a circular pattern. Two things that are most conspicuous by their absence of faults are the two white arcs. The solid white arc is the path of the Feather River Valley, and is reflected in the lineaments both north west and southeast of the arc. While there are a few isolated expressions of faults, with a valley this large, it might be expected that faults would occur the entire length. Without faults, the assumption might be that the river itself had to erode the entire depth of the valley, but the parallel lineaments suggest a structural cause. The broken white arc does have several internal faults seemingly concentric to it, but although there are a couple faults on the south edge, the majority of the arc is without fault expression. The same is true of the major valley that runs up the center, the dotted line parallel with trend 8.

Without expression in faults, how do major valleys form? Release-wave valleys (Barnhart 2017) are a viable option.

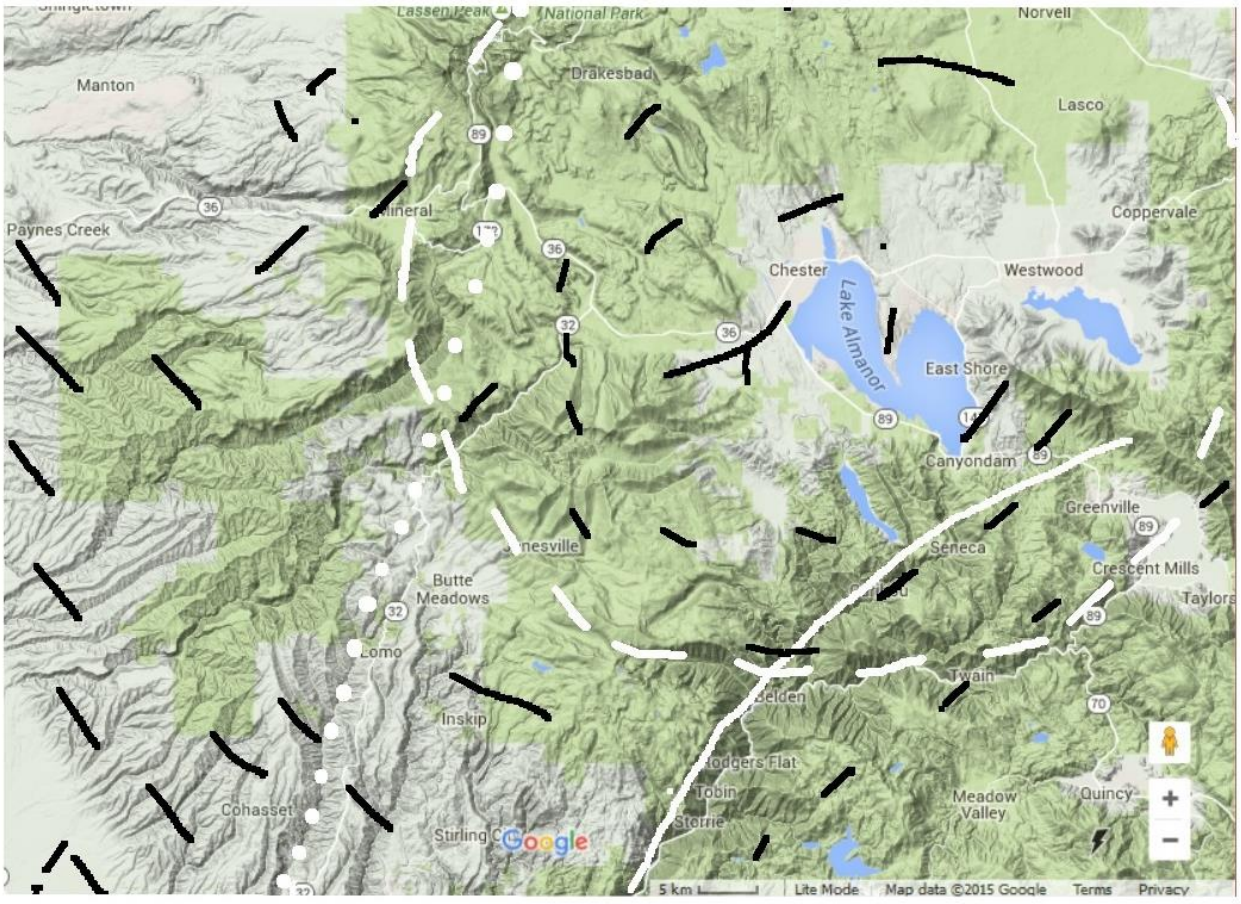

Figure 6.11. Google Earth Terrain map of same area as Figure 6.10 showing the major faults and fault trends. White lines emphasize the lack of faults in these two arcuate lineaments and central valley. (After Gutierrez et al. 2010.)

Williams to Dunnigan section of the Coastal Range

Coastal Range

Rocks of the Coastal Range are grouped into the Franciscan Complex. DeCourten (2015, page 5) connects these to accreting "seamounts, island arcs, coral reefs, and small continental blocks that were carried on subducting ocean plates colliding with the western edge of the continent and were embedded into the existing margin."

If accretion is their origin, then we would expect to see lineaments parallel to the coast to be most prominent. But while Figure 6.12 shows trends 1 and 2 to be well represented, they are no more so than the other six trends.


Colusa
Arbuckle
College C
Buck Island
Rumsey
D
1
Google earth
© 2015 Google
Tour Guide
Imagery Date: 7/10/2013 38°59'19.93" N 122°11'40.24" W elev 899 ft eye alt 21.57 mi


Colusa
Arbuckle
College C
Buck Island
Rumsey
D
2
Google earth
© 2015 Google
Tour Guide
Imagery Date: 7/10/2013 38°59'19.93" N 122°11'40.24" W elev 899 ft eye alt 21.57 mi


Colusa
x
Arbuckle
College C
Buck Island
3
Rumsey
D
Google earth
© 2015 Google
Tour Guide
Imagery Date: 7/10/2013 38°59'19.93" N 122°11'40.24" W elev 899 ft eye alt 21.57 mi

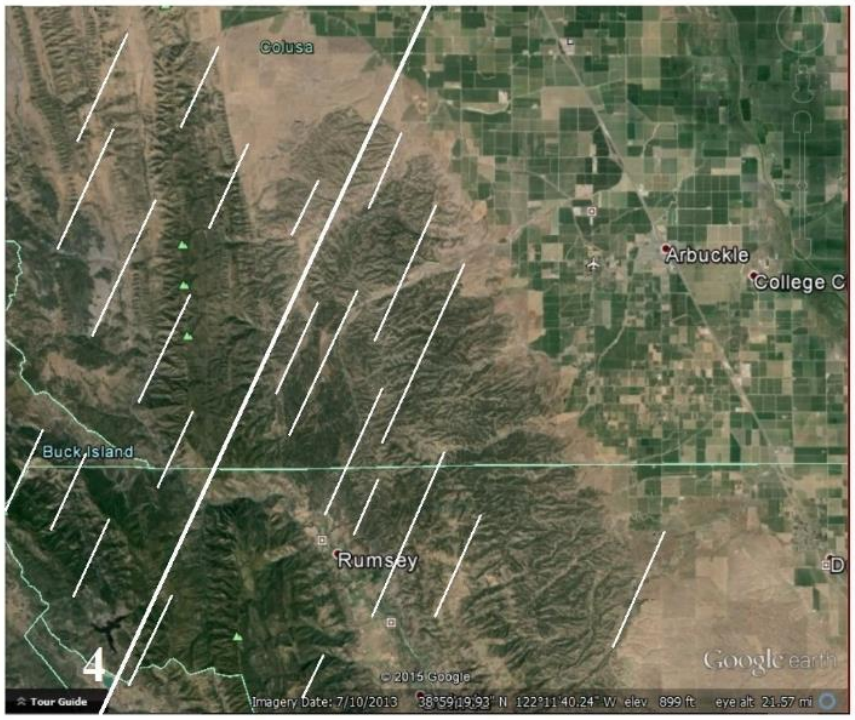
Colusa
Arbuckle
College C
Buck Island
Rumsey
D
4
Google earth
© 2015 Google
Tour Guide
Imagery Date: 7/10/2013 38°59'19.93" N 122°11'40.24" W elev 899 ft eye alt 21.57 mi


Colusa
Arbuckle
College C
Buck Island
Rumsey
D
5
Google earth
© 2015 Google
Tour Guide
Imagery Date: 7/10/2013 38°59'19.93" N 122°11'40.24" W elev 899 ft eye alt 21.57 mi

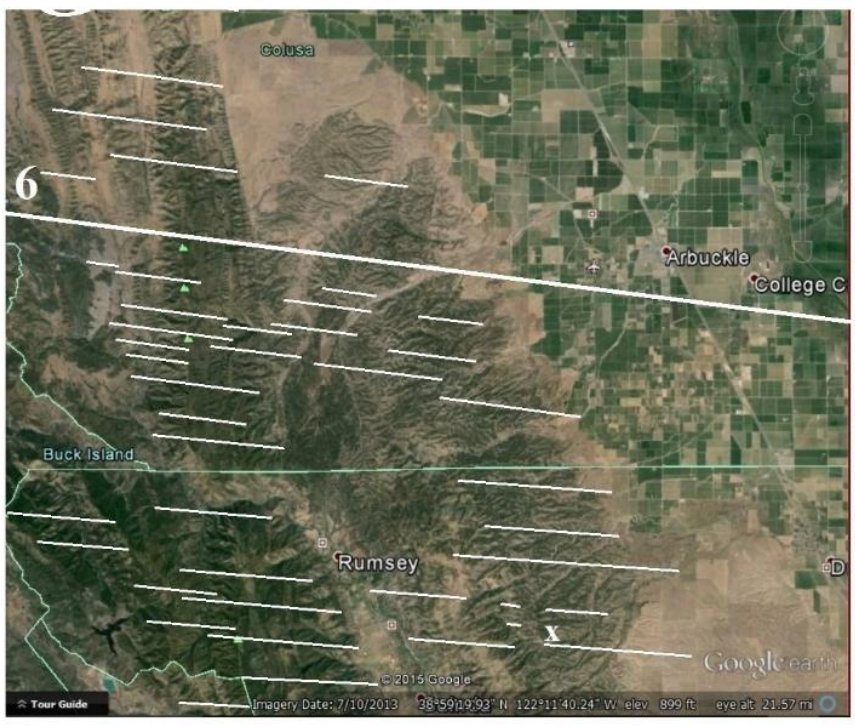
Colusa
6
Arbuckle
College C
Buck Island
Rumsey
D
x
Google earth
© 2015 Google
Tour Guide
Imagery Date: 7/10/2013 38°59'19.93" N 122°11'40.24" W elev 899 ft eye alt 21.57 mi

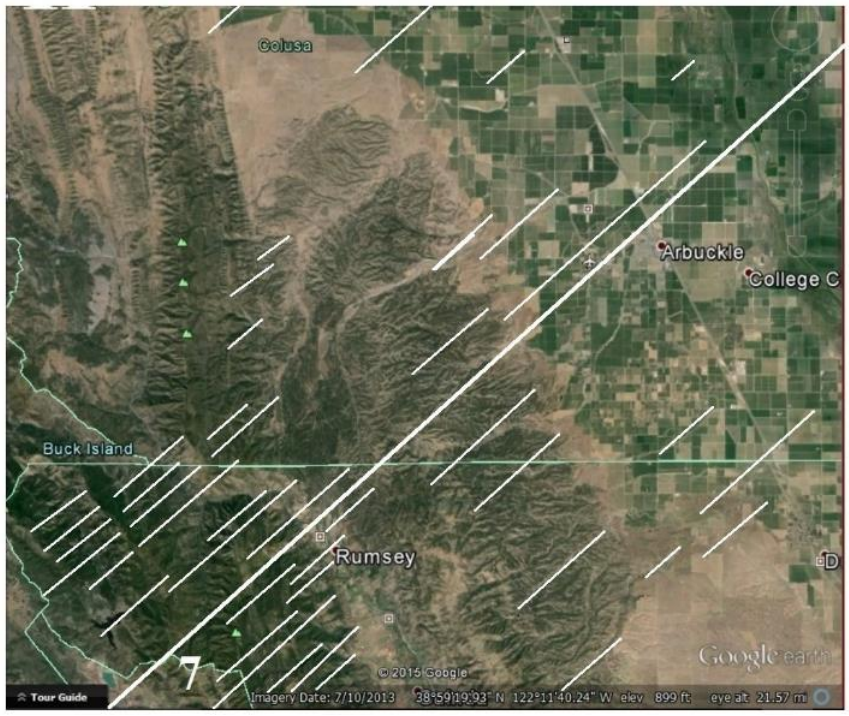

Figure 6.12. Google Earth image of Williams to Dunnigan section of the Coastal Range. Image shows only the inner portion of that range to allow a more detailed view. Images 6.17.1- 6.17.8 explanations consistent with Figure 6.3. (2013. 38°59'19.93"N, 122°11'40.2"W, accessed 10 November 2015.)

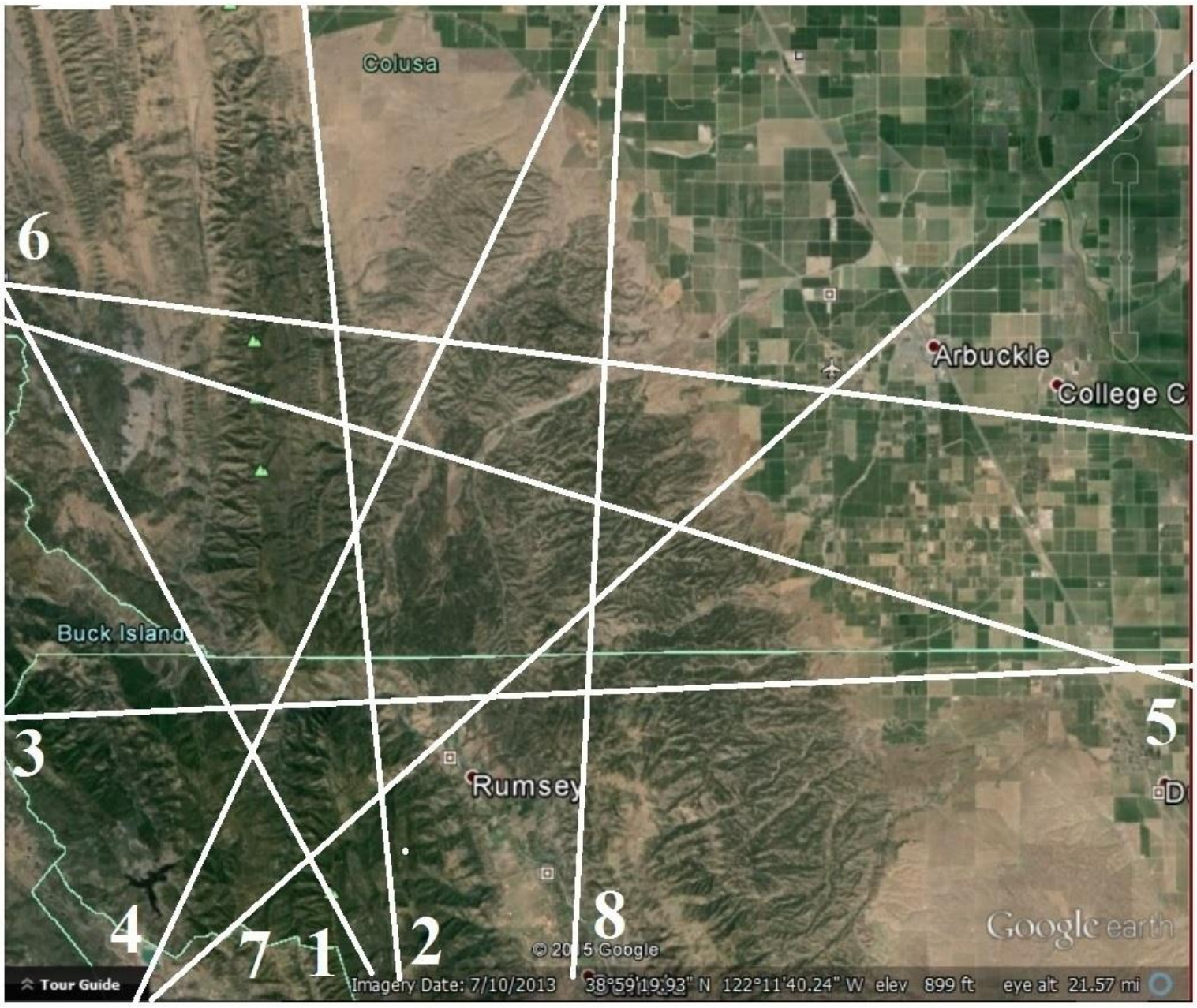

Figure 6.13. Google Earth image of Williams to Dunnigan showing a compilation of all 8 trends in one image for comparison. (2013, same as Figure 12.)

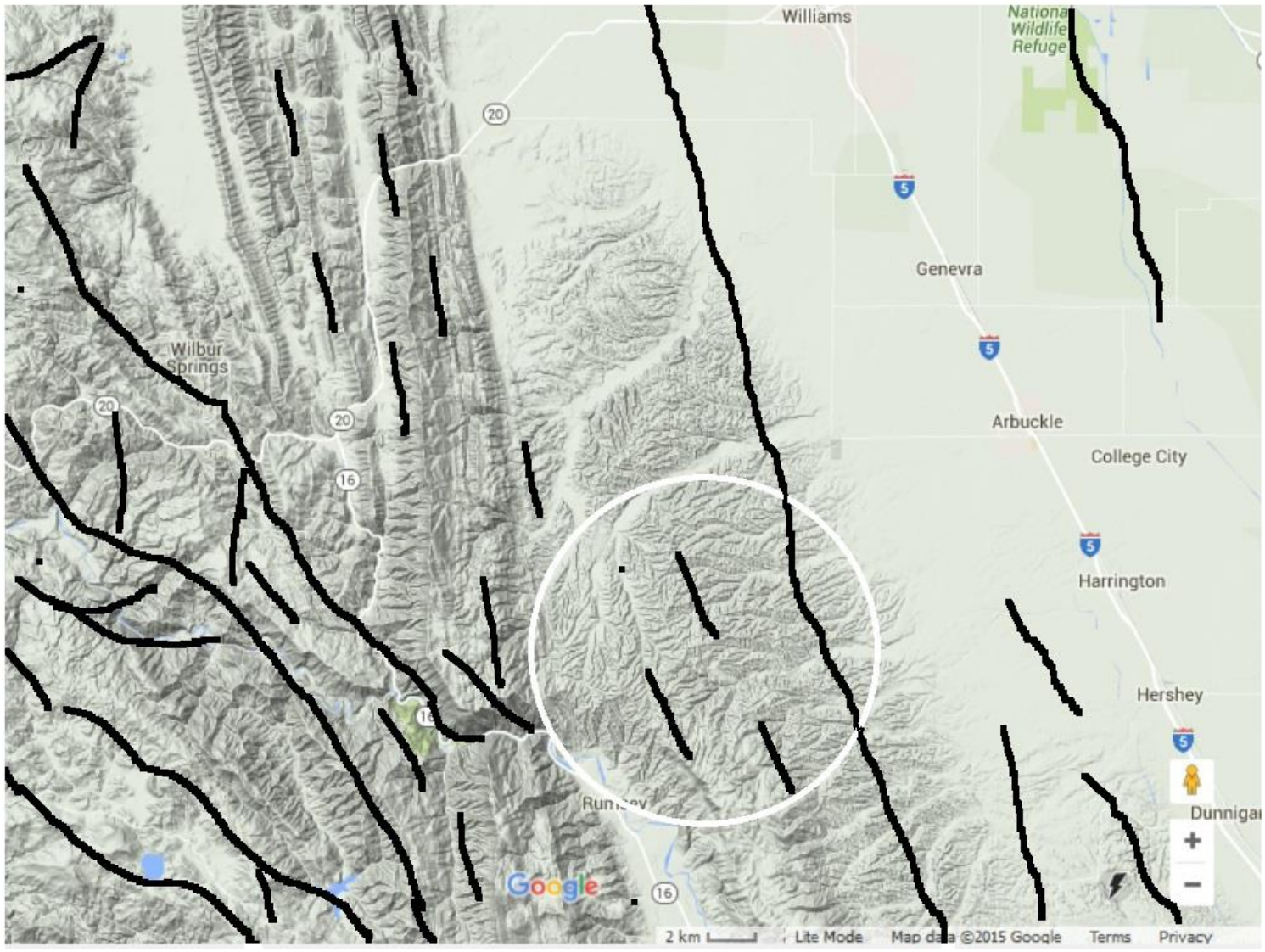

Figure 6.14: Google Earth Terrain map of same area as Figure 13 showing the major and many minor mapped faults and fault trends, after Gutierrez et al. 2010.

The faults charted in Figure 6.14 show a clear change of rock direction from trend 1 on the far west to trend 2 in the central area. But while this relationship seems apparent in the terrane map, it is not at all prominent in the Landsat images of Figure 12. As the view in Figure 15 shows ridges aligned with trend 3, the ridge from which they all arise is aligned with trend 2. It is almost as if the rocks were all in place but plastic, and a lineament spread its energy over them all at once, getting a differently shaped response depending on its cumulative interaction with other linears in the vicinity. The supposed direction of accretion was certainly not the only direction of force acting on the area. But neither did each of the trends push mountains up. Some are more expressed in linears involving gullies and ridges (release wave valleys?).

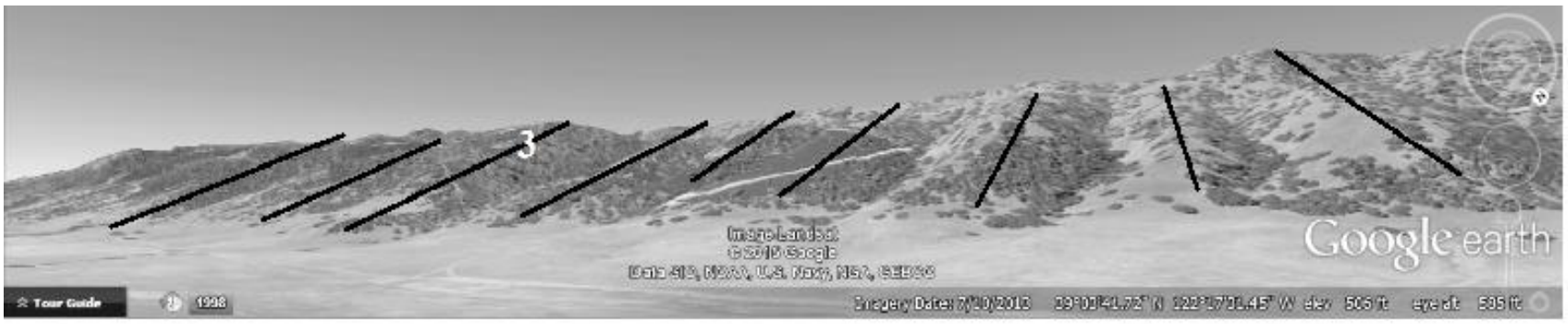

Figure 6.15. Google Earth Topographic drape from Figure 6.12.3, point x, looking to the southwest. Note the repeated arrangement of all midground ridges in alignment with trend 3, while top of ridge is trend 2. (2013. 39°03’41.72”N, 122°17’31.45”W, accessed 12 November 2015.)

Figure 6.16, viewing west from X in Figure 12.6, trend of parallel ridges in mid and foreground align with trend 6, and ridge is another unmapped trend.

Figure 6.16. Google Earth Topographic drape from Figure 12.6, point x, looking due west. Note the grouping of ridges and gullies. In the fore and midground ridges align with trend 6, while the background ridges move to the left. These background ridges are parallel, not quite as steeply angles as trend 7, and not plotted. (2015, 38˚50'47.61"N, 122˚06'48.35"W, accessed 14 November 2015.)

Many of the sedimentary strata in this area are tilted upwards (Figure 17) as trend 8, but trend 3's linears cut through them as if they were not there to form ridges and gullies. This confirms, some linears are stronger than others.

Figure 6.17. Google Earth topographic drape of hills, almost due west of the center of Figure 6.12.8, labeled point x. View is to the west with the general direction of the exposed strata aligned with trend 8. Three strata are partially traced with arrows; one-sided right, two-sided right, and one-sided left. By contrast to the direction of the strata, the major ridges visible are aligned with megashear or trend 3, including the long ridge terminating in the lower right corner. (2013, 38˚57'56.02"N, 122˚18'24.55"W, accessed 12 November 2013.)

It is observed, the lowest saddles draining through the last hills of the Coastal Range, Figure 6.12.7, do follow megashear 7, but not the highest saddles. Although parallel lineations themselves, they consistently follow another megashear not mapped. Trend 7 continues to be represented in low ridges and streams of the Central Valley area, the only trend primary doing so.

Discussion, Conclusion

Lineaments are traced in Google Earth where cultivation and vegetation do not obscure the original surface. Photogeology has grown up considerably since the mid 1940's when the first aerial photos became commonly available. Photogeologist concentrating on limited areas; a depositional basin, mining claim, or oil play recognized 3-4 trends in all areas, but we have traced 8 over most of California from the Pacific Coast to the Sierra Nevada Mountains. Google Earth makes this possible for the land surfaces and sonar and gravity anomaly extend it across ocean basins. Once the trend has been mapped over a sufficient distance the theoretical center can be mathematically determined. Many trends can be traced in ever decreasing Small Circles to their centers (Chapter 2). Once finding a common center, a logical argument can be made for a common genesis for all of a trend's linears no matter how far away they occur from that center, and geomorphic effects they are involved with.

Concentric Global Ring Structures (CGRS) provide a form consistent with lineaments representing ridges and valleys as in the Pacific Fracture Zones. Aligned and parallel trends of mountain and valley displayed by erosion patterns would be a predicted result, as demonstrated throughout California. Linear erosion paths, especially release-wave valleys down mountain courses will be eventually claimed by rivers for their paths, but *not* formed by the river.

If overlapping trends give a sense of relative timing to the mountains and valleys involved, by extension, the sediments therein have the same connection with that timeframe, whether depositional near the center or distorted at a distance. This means the rock record, and by extension the fossil record, becomes an impact record which cannot be globally continuous as impacts are all local and episodic.

At first, it might seem confusing to try to deal with so many directions of force in a single area, Figure 6.18, but this paper has shown that at closer distance (Figure 6.1) many lineaments are even more visible, helping us understand how multiple CGRS shaped the geomorphology.

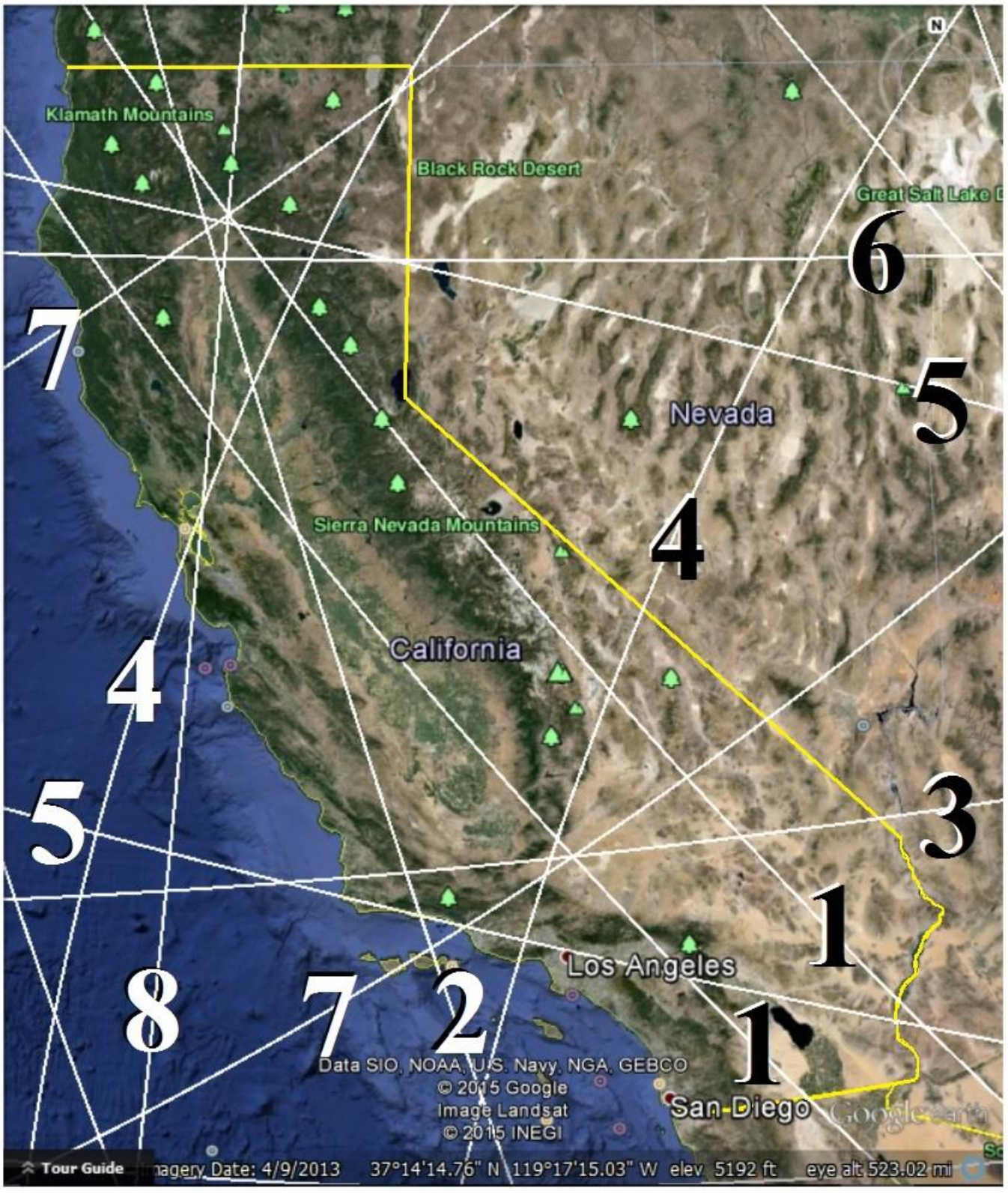

Figure 6.18. Google Earth image of California showing major expressions of the CGRS lineaments used in this paper. (2013. 37˚14’14.76”N, 119˚17’15.03”W, accessed 18 December 2015.)

If circular and straight/ slightly curvilinear lineaments are ubiquitous and highly visible, it follows that their occurrence is at the top of the rock record requires them to be of recent genesis, and their erosional events, extending to the size of California, to be *more* recent.

While Griffith (1924), posited that existing cracks and flaws would initiate fractures, and Hoek (1964) assumed bedding planes in sedimentary rock provided the strongest expression of those flaws, this paper finds that major lineations ignore bedding planes and existing faults do not account for many lineament’s direction. As fracturing of rock is analyzed to occur along plains axial to stress/ strain or perpendicular with lateral strain, with other directions requiring inducement (Hoek and Martin 2014), this paper is showing, a primary inducement for all fracture initiation and propagation is CGRS and the stresses fostered on the terrane by impacts.

I find as the centers of CGRS occur far from their expression, Gay (2012) suggestion that linears are connected with joints faults and probably often connected to the basement to have real merit for the distant linears. But by contrast, with the smaller circular lineaments, with centers only a few kilometers away, their trends may not extend to the basement.

The mapped centers for the eight recognized CGRS in this paper, are identified and tentatively named in Table 1.

Lineament # this paper	Tentative Name	Location	Center located:
1	Great Bight	Lat -51.733273° Lon 125.416700°	Great Australian Bight between Antarctica and mainland
2	Verde	Lat 16.354025° Lon -24.121064°	Near the Cape Verde Islands, Atlantic Ocean
3	Pacific	Lat 72.708453° Lon 78.032992°	Yenisei Bay, Kara Sea, Siberia
4	Gulf of Mexico	Lat 23.123490° Lon -89.603740°	Yucatan Shelf in the middle of Gulf of Mexico.
5	Tver	Lat 56.797161° Lon 35.896931°	150 km north of Moscow, Russia, near city of Tver.
6	North Pole	Lat 89.617820° Lon -21.218272°	45 km south of North Pole towards Greenland.
7	Bering Sea	Lat 62.883332° Lon -177.933333°	Center of arc formed by Aleution Islands, Bering Sea
8	Ascension	Lat -10.967566° Lon -12.239272°	On the edge of the Ascension Fracture Zone, Atlantic Ocean

Table 6.1: Concentric Global Ring Structures associated with lineaments in this paper, with tentative names and approximate centers.

Acknowledgements

Deepest thanks to Maarten ‘t Hart, who wrote the overlay program for Google Earth to plot the CGRS and mathematically calculate their centers. Without his helpful tool, this understanding of what these lineaments represent would never have happened. “The second angel blew his trumpet, and something like a great mountain, burning with fire, was thrown into the sea, and a third of the sea became blood” (Revelations 8:8 ESV).

References.

Barnhart, W.R. 2017. Finding a cause in Earth’s lineaments. *Creation Research Society Quarterly*. 53: 191-205.

DeCourten, F. 2015. *Geology of Northern California*. Cengage Learning. http://www.cengage.com/custom/regional_geology.bak/data/DeCourten_0495763829_LowRes_New.pdf . Accessed 21 December 2015.

Gay, S.P. 2012. Joints, Linears, and Lineaments – The basement connection. *Search and Discovery Article #41083.* http://www.searchanddiscovery.com/pdfz/documents/2012/41083gay/ndx_gay.pdf.html Accessed 07/13/2016.

Griffith A.A. 1924. Theory of rupture, *Proceedings of the First International Congress of Applied Mechanics, Delft:n Technische Boekhandel and Drukkerij*, Bienzo and Burger (Editors):55-63.

Gutierrez, C., Bryant, W., Saucedo, G., and Wills, C. 2010. California geologic data map series map no. 2 – Geologic map of California. California Geological Survey. Scale 1:750,000.

Hodgson, R.A. 1961. Regional study of jointing in Comb Ridge-Navajo Mountain area, Arizona and Utah*: AAPG Bulletin,* v. 45/1, p.1-38,

Hoek, E. 1964. Fracturing of anisotropic rock. *Journal of the South African Institute of Mining and Metallurgy* 64 (10):501-518.

Hoek, E. and Martin, C.D. 2014. Fracture initiation and propagation in intact rock – A review. *Journal of Mechanics and Geotechnical Engineering* 6:287-300.

O’Driscoll, E.S.T. 1983. Deep Tectonic foundations of the Eromanga Basin. Australian Petroleum Exploration Association Conference, March 6-9 1983. *The APEA Journal* 23(1):5-17.

Tirén, S. 2010. Lineament interpretation short review and methodology. *GEOSIGMA AB*. Report 2010:33, 42 pages.

Wampole, J. 2006. *Simplified Geologic Map of California: Map sheet 57*. California Department of Conservation, California Geologic Survey. Scale approx. 1:2,250,000.